ENVIRONMENTAL RESEARCH
LETTERS

LETTER

Strong influence of convective heat transfer efficiency on the cooling benefits of green roof irrigation

Linying Wang[1], **Maoyi Huang**[2,3] **and Dan Li**[1,*]

[1] Department of Earth and Environment, Boston University, Boston, MA 02215, United States of America
[2] Atmospheric Sciences and Global Change Division, Pacific Northwest National Laboratory, P.O. Box 999, Richland, WA 99352, United States of America
[3] Now at Office of Science and Technology Integration, National Weather Service, National Oceanic and Atmospheric Administration, Silver Spring, MD 20910, United States of America
* Author to whom any correspondence should be addressed.

E-mail: lidan@bu.edu

Keywords: green roofs, irrigation, urban heat mitigation, surface energy balance, convective heat transfer, earth system model

Supplementary material for this article is available online

OPEN ACCESS

RECEIVED
19 July 2020

REVISED
25 July 2021

ACCEPTED FOR PUBLICATION
29 July 2021

PUBLISHED
10 August 2021

Abstract

By enhancing evapotranspiration (ET), green roofs provide cooling benefits for the urban environment and are recognized as a promising heat mitigation strategy. The evaporative cooling effects of green roofs strongly depend on the soil moisture conditions and thus irrigation may be needed to sustain the cooling benefits. It has been shown that the magnitude of cooling benefits offered by green roof irrigation varies spatially, but its controlling factors remain elusive. In this study, we combine a surface energy balance (SEB) model with global simulations generated by an improved Earth System Model to illustrate the key factors controlling the cooling benefits of green roof irrigation. We employ a simple irrigation scheme, which is only active when there is no ice in soil layers and when the soil moisture is below field capacity. As a result, most of the irrigation water leaves the green roof system via ET. We find that the magnitude and also the spatial variability of the cooling benefits of green roof irrigation are controlled by the irrigation amount, and a surface energy redistribution factor that encodes the efficiencies of different SEB components in transferring heat. Further analysis indicates that the enhancement of latent heat flux due to irrigation is largely balanced by the reduction of sensible heat flux on green roofs. Therefore, the amount of irrigation needed per unit decrease of green roof surface temperature is mainly controlled by the convective heat transfer efficiency. A lower convective heat transfer efficiency (e.g. under a lower wind speed) helps reduce the amount of irrigation needed per unit decrease of green roof surface temperature. This study highlights the importance of SEB in constraining the cooling benefits of green roof irrigation and provides valuable guidance for urban planners and policy makers in terms of heat mitigation and sustainable water management.

1. Introduction

The conversion of vegetated to impervious surfaces in urban environments leads to reductions in evapotranspiration (ET) and contributes to many environmental issues such as urban heat islands and urban flooding (Oke *et al* 2017). Given the compact nature of urban areas and limited available space for plants and trees, green roofs are recognized as a promising strategy for reducing urban heat and mitigating urban flooding, especially in high-density cities (Tsang and Jim 2011, Ng *et al* 2012, Georgescu *et al* 2014, Santamouris 2014, Georgescu 2015, Estrada *et al* 2017). Green roofs can also modulate the urban boundary layer conditions via land-atmosphere interactions, which might affect the local and regional air quality (Sharma *et al* 2016, Song *et al* 2018). Over the last two decades green roofs have been studied and implemented in many cities and countries (Wong *et al* 2003, Gaffin *et al* 2009, Smith and Roebber 2011, Zinzi and

Agnoli 2012, Gagliano *et al* 2016, Shafique *et al* 2018, WGIN 2021).

Green roofs, also known as eco-roofs or living roofs, are typically composed of vegetation, soil substrate, filter, drainage, root barrier, and waterproofing membrane (Scholz-Barth and Tanner 2004, Besir and Cuce 2018, Shafique *et al* 2018). As an important heat mitigation strategy, the effectiveness of green roofs is largely controlled by soil water availability. At point scales, observational and modelling studies have shown that ET and the evaporative cooling effects of green roofs are strongly dependent on soil moisture conditions (DiGiovanni *et al* 2013, Sun *et al* 2014, William *et al* 2016, Heusinger *et al* 2018). That is, green roofs can reduce the surface and near-surface air temperatures when they are wet; however, their cooling benefits greatly diminish when they are dry. These findings are corroborated by numerical studies at city scales (Li *et al* 2014, Sun *et al* 2016). Therefore, irrigation might be needed to sustain the cooling effects of green roofs, especially in dry regions (Van Mechelen *et al* 2015, Chagolla-Aranda *et al* 2017, He *et al* 2017, Yang and Wang 2017). The availability of water is also important for the healthy growth of vegetation on green roofs (Qin *et al* 2016, Tsang and Jim 2016).

To explicitly quantify the relation between the cooling benefit and the irrigation amount for urban green infrastructure that includes but is not limited to green roofs, previous studies have predominately relied on numerical weather prediction models such as the Weather Research and Forecasting (WRF) model (e.g. Vahmani and Hogue 2015; Wang *et al* 2019) coupled with improved irrigation and other hydrological parameterizations (Wang *et al* 2013, Vahmani and Hogue 2014, Yang and Wang 2015, Yang *et al* 2015), as well as building energy models (Sailor 2008, Heusinger *et al* 2018). For example, a recent study by Wang *et al* (2019) quantified the cooling effects of irrigating urban vegetation on the ground (not on the roof) over the Contiguous United States (CONUS) using a metric called urban water capacity, which is calculated as the daily average irrigation depth per degree of urban temperature reduction. Their results showed that the values of urban water capacity are 4.52 ± 0.77 mm d^{-1} $°C^{-1}$ and 7.27 ± 1.27 mm d^{-1} $°C^{-1}$ (mean $\pm$ standard deviation) for surface and near-surface (commonly defined as 2 m above the displacement height) air cooling, respectively, over the CONUS. The values of urban water capacity for surface cooling range from 3.01 ± 0.39 mm d^{-1} $°C^{-1}$ to 5.01 ± 0.37 mm d^{-1} $°C^{-1}$ across the eight climate regions defined in Wang *et al* (2019). The cooling benefits of urban irrigation have also been examined from the perspective of tradeoff between heat mitigation and water conservation (Epstein *et al* 2017, He *et al* 2017, Vahmani and Jones 2017, Yang and Wang 2017). For example, also using the WRF model, Vahmani and Jones (2017) showed that the implementation of cool roofs in California leads to reductions in both the urban temperature and the water use for irrigating urban vegetation on the ground. In other words, the irrigation needed at a given urban temperature could be partly saved if the urban temperature was reduced through other heat mitigation strategies (e.g. cool roofs).

An important question that remains to be answered is that what fundamentally controls the magnitude of cooling benefits of green infrastructure irrigation, which motivates this study. Here we focus on green roof irrigation, which is less studied compared to irrigation for urban vegetation on the ground. Unlike previous modelling studies that focus on developing detailed parameterizations for green roofs including irrigation schemes, we use a global Earth System Model with a customized green roof parameterization that allows irrigation, aided by a simple surface energy balance (SEB) model, to illustrate the key drivers of the cooling benefits of green roof irrigation. Our aim is not to predict the water use of green roofs globally, but rather to demonstrate the impact of green roof irrigation on surface temperature from the perspective of how the SEB is altered as a result of watering.

2. Methods

2.1. Earth system modelling

2.1.1. Green roof parameterization in CESM

We perform numerical experiments with the Community Land Model version 5 (Lawrence *et al* 2019), which is the land component of the Community Earth System Model version 2 (CESM2) (Danabasoglu *et al* 2020) and includes an urban model called the Community Land Model Urban (CLMU). The CLMU has a roof module that handles the energy and water balances over roof surfaces. It also considers other facets such as walls, and impervious/pervious ground in the urban canyon. Details about the CLMU model can be found elsewhere (Oleson *et al* 2008a, 2008b, 2011, Oleson 2012, Oleson and Feddema 2020). The default CLMU does not have a parameterization scheme for green roofs and thus we add a green roof module to CLMU. We first separate the roof component within CLMU into three types: the regular roof, the white roof, and the green roof. The momentum, energy, as well as water fluxes between the roof and the air are weighted averages of those from the regular roof, the white roof, and the green roof. The model always calculates the temperatures and fluxes for each roof type even if the fraction of a certain roof type (e.g. white roof) is zero, but the atmosphere does not receive the fluxes from this particular roof type under such conditions. In this study, we only consider regular and green roofs, with the white roof fraction set to zero.

In the green roof module, the green roofs are treated as a three-part system: vegetation, soil and roof deck. The treatment of the roof deck is identical to that in the original CLMU model, or that of the regular roof, and the treatment of soil follows the treatment of pervious ground in the urban canyon (Oleson *et al* 2008a). The soil substrate of the green roof is represented by 20 layers, and the associated hydrology includes processes like infiltration, runoff generation, as well as the soil water dynamics. Compared to the regular roof and the pervious ground, the uniqueness of the green roof system is that it considers the heat transfer between the soil and the roof deck. In order to archive this, the heat conduction equation is solved simultaneously for the soil and the roof deck. In addition, we parameterize the impact of vegetation on ET through the stomatal resistance concept (see text S1 (available online at stacks.iop.org/ERL/16/084062/mmedia)), with the stomatal resistance of vegetation parameterized using the so-called Jarvis scheme (Jarvis *et al* 1976).

Our parameterization also includes an irrigation option for green roofs. When irrigation is turned on, the green roof is irrigated when any of the soil layers has a soil moisture value (θ) below the field capacity (θ_{fc}). When there exists ice in the green roof soil layers, no irrigation is applied. The amount of irrigation water applied to green roofs is calculated as the sum of soil water deficits (i.e. $\theta_{fc} - \theta$) in all soil layers.

Compared to regular roofs whose input parameters such as albedo come from a global dataset (Jackson *et al* 2010), the extra input parameters for the green roof system (and their data sources) are listed in table S1, including green roof albedo, green roof emissivity, soil depth, soil texture, hydrological parameters, and plant physiological parameters needed by the stomatal resistance parameterization. These properties are determined either using typical values from the literature (Sun *et al* 2013, Wang *et al* 2013, Van Heerwaarden and Teuling 2014, Tian *et al* 2017) or based on practical ranges reported in literatures. Also note that the Jarvis scheme is empirical and the parameters do not change temporally. The values of these parameters can be adjusted by users and spatially varying values can be also used. We have performed extensive sensitivity studies to these green roof parameters and found that changes in the SEB as well as the evaporative cooling benefits of green roof irrigation vary with these parameters (not shown), which is consistent with previous studies (Sailor 2008). However, the main finding of this study, i.e. the strong influence of the convective heat transfer efficiency on the cooling benefits of green roof irrigation, is not affected by the exact values of these parameters (within reasonable ranges).

2.1.2. Model evaluation

In this section, we evaluate the green roof module implemented into CESM using observations from an experimental site at the campus of Tsinghua University, Beijing, China (116.35° E, 40.05° N) in July 2011 (Sun *et al* 2013). The green roof at the Tsinghua University site is located on a 11 m tall, multi-functional office building and is composed of a vegetation-soil layer (0.05 m) and a medium layer (0.15 m) on top of the concrete roof deck. The vegetation is *Sedum lineare* (or *S. lineare*), which is an evergreen succulent plant and very common on green roofs (Scholz-Barth and Tanner 2004). The meteorological variables, including precipitation, air temperature, relative humidity, atmospheric pressure, wind speed and direction, and incoming shortwave and longwave radiation are recorded by a CR1000 data logger (Campbell Scientific) and then averaged at hourly intervals. The green roof surface temperature and soil water content are also measured, which are used to evaluate the model performance. Specifically, the green roof surface temperature is measured by an infrared sensor above the vegetation-soil layer and the soil water content is measured by a time domain reflectometer sensor located in the medium layer. More details about the site and instruments can be found in Sun *et al* (2013).

We run the CESM model at a single-point over the grid cell (116.3° E, 40° N) at a horizontal resolution of 0.1°. The model is uncoupled from the atmospheric model and is forced by the hourly-averaged meteorological observations, which is applied at 2 m above the urban canopy. The input surface dataset specified for this site is created using the CLM tool (https://escomp.github.io/ctsm-docs/versions/release-clm5.0/html/users_guide/using-clm-tools/creating-surface-datasets.html). The initial states of green roof soil temperature and moisture are assumed to be uniform across the entire depth of the green roof, with values taken from the *in situ* measurements. The green roof thermal and hydraulic parameters are principally adopted from the study by Sun *et al* (2013) (see table S2). Here we emphasize that some parameters are unique for this site and are different from those used in global runs (to be discussed in the following section), especially the soil-related parameters. In global runs, the hydraulic properties of the soil are determined by the soil hydrological parameterization in CESM once the fractions of clay and sand are given. However, since the soil hydrological parameterization in CESM might not capture the soil characteristics at this particular site, we use the values in table S2 for the soil hydraulic parameters at this site. The same applies to the thermal properties of the vegetation-soil and medium layers and the roof deck.

The validation period is chosen to be 2–20 July 2011, during which the site experienced both drying-down and rainfall periods, and no irrigation was applied. Comparisons between the CESM-simulated and measured green roof surface temperature (T_s) and soil water content (θ) are shown in figure 1.

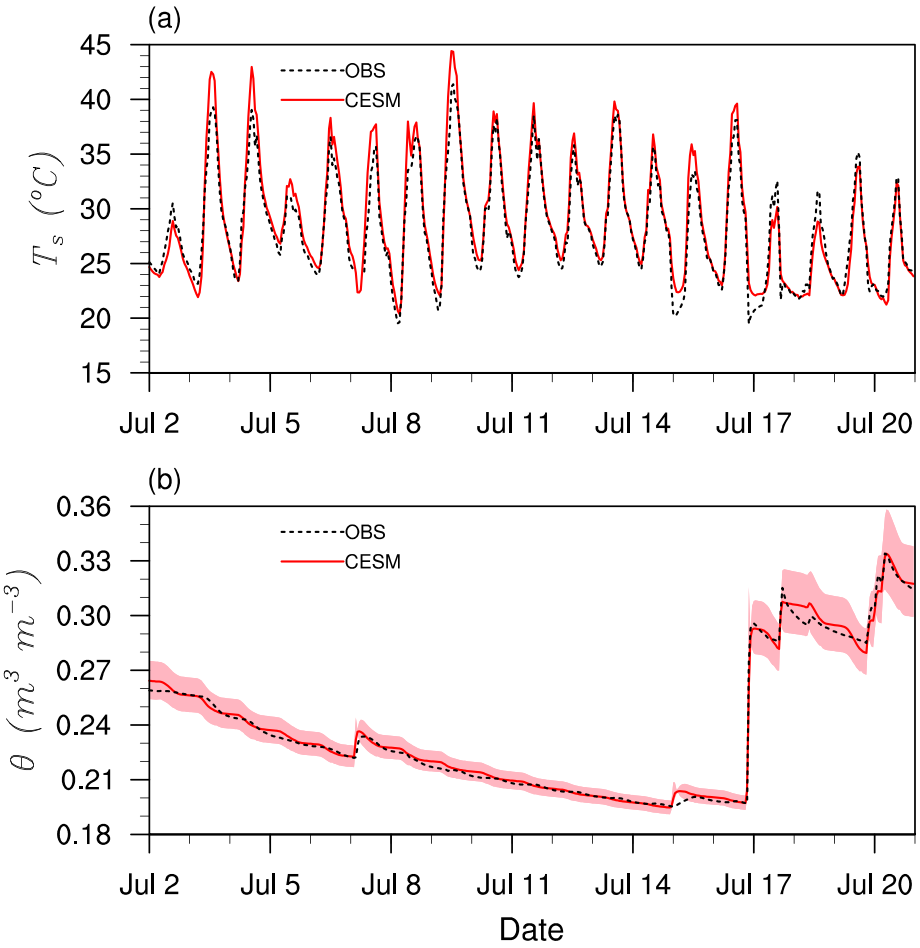

Figure 1. Comparison of observed and CESM simulated (a) green roof surface temperature (T_s), with R^2 of 0.95 and RMSE of 1.38 °C, (b) volumetric soil water content (θ), with R^2 of 0.995 and a RMSE of 0.0028 m^3 m^{-3}, during 2–20 July 2011. In (b), the red line is the multi-layer mean soil moisture and the shadow is the range of soil moisture across different layers. The *in situ* observations (OBS) are measured at the experimental site on the campus of Tsinghua University, Beijing, China.

The CESM-simulated T_s agrees well with the observation, with a R^2 of 0.95 and a RMSE of 1.38 °C. We also compare the simulated multi-layer mean soil water content as well as its range (i.e. maximum and minimum values) with the measurements, and find that the model can also capture the dynamics of soil water content, with a R^2 of 0.995 and a RMSE of 0.0028 m^3 m^{-3}. In summary, the green roof module implemented into the CESM model is capable of capturing the observed hydrothermal dynamics of green roofs at this site. We thus use the improved CESM model with the green roof module to further investigate the impacts of green roof irrigation at global scales.

2.1.3. Global experiments

Based on an initial condition provided by the default CESM codes (which has been spun up), we run the model at a horizontal resolution of 0.9° latitude × 1.25° longitude with 0% green roof for another 84 years by recycling the 1990–2010 Global Soil Wetness Project Phase 3 atmospheric forcing (Lawrence *et al* 2019) four times until the land state variables reach a new equilibrium. The default CESM codes do not include the green roof parameterization and hence there is no information for the green roof in the provided initial condition. As a result, we use the information for the pervious ground as the initial state for the green roof in this spin up run. During the spin up run, the green roof develops its own dynamics encoded by the green roof parameterization. All simulations conducted in this study (table S3) use the same initial condition resulting from this 84 year spin up run. In the land-only (uncoupled to an active atmospheric model) simulations, we perform three 21 year numerical experiments using the same atmospheric forcing from 1990 to 2010 and analyse the last 20 years of simulation results. In the control (CTL) case, there is 0% green roof (see table S3). We also conduct another two sensitivity experiments with 100% green roofs (Case_Noirrigation and Case_Irrigation, table S3). In Case_Noirrigation, the green roof is not irrigated while it is irrigated in Case_Irrigation. It should be noted that land-only simulations do not imply that the near-surface air temperature (air temperature at 2 m above the displacement height, hereinafter 2 m air temperature) is the same, since the atmospheric forcing is applied at

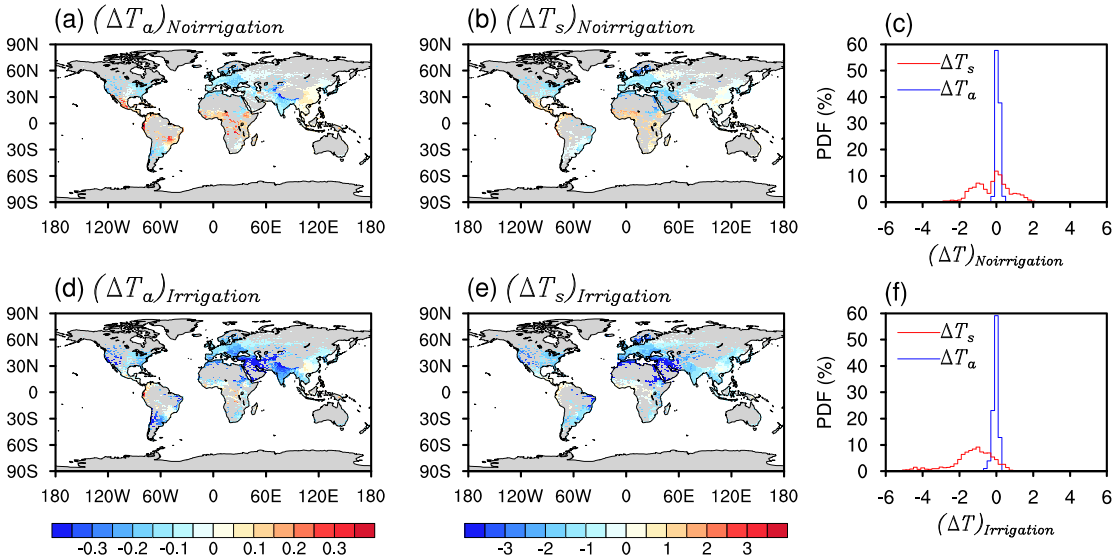

Figure 2. The cooling effects of non-irrigated and well-irrigated green roofs simulated by CESM. (a) The differences in terms of 2 m air temperature between Case_Noirrigation and CTL, (b) the surface temperature differences between green and regular roofs in Case_Noirrigation, (d) the differences in terms of 2 m air temperature between Case_Irrigation and CTL, (e) the surface temperature differences between green and regular roofs in Case_Irrigation. Also shown are the probability density functions (c) and (f). All units for temperature are K. The results are the annual daily mean over 20 years (1991–2010) from land-only simulations. Only grid cells with more than 0.1% of urban land are shown.

30 m above the urban canopy. The 2 m air temperature in these land-only simulations still respond to the adoption of green roofs (figure 2). However, these land-only simulations preclude any feedbacks in the boundary layer and above as well as ocean and sea-ice feedbacks.

In addition to land-only simulations, two land-atmosphere coupled simulations (with and without irrigation) are conducted (hereafter Case_Noirrigation_LA and Case_Irrigation_LA, see table S3). The atmospheric model used in these land-atmosphere coupled simulations is the Community Atmosphere Model version 6, which is the atmosphere component of CESM2. The land-atmosphere coupled simulation follows the Atmospheric Model Intercomparison Project protocol for the historical period (Gates *et al* 1999) and uses prescribed sea surface temperatures, solar variations and aerosol chemistry from 1990 to 2010. We treat the first year as further spin up for the atmospheric model, and the analysis focuses on the period 1991–2010 (identical to land-only simulations).

For all simulations, we output the daily mean roof surface temperatures and all fluxes, including incoming and outgoing shortwave and longwave radiation, sensible heat flux, latent heat flux, and ground heat flux associated with green roofs. We also output the daily mean aerodynamic resistance, heat capacity, and thermal conductivity for green roofs, as well as the pressure, air density, and 2 m air temperature for the urban land. These daily mean outputs are used for our analysis throughout the paper. We note that the urban extent in CLMU is represented by three urban density classes: tall building district (TBD), high density (HD), and medium density (MD). For each grid cell, the urban model output is a weighted average of the output for individual classes. In this paper, we only show results for grid cells in which urban land is more than 0.1% (i.e. the sum of TBD, HD, and MD needs to be larger than 0.1%).

2.2. A simple SEB model

To understand how the green roof surface temperature responds to irrigation, we develop a simple SEB model building on earlier work (Bateni and Entekhabi 2012). This SEB model is not used as a predictive model, but rather used as a diagnostic tool to illustrate how green roof irrigation alters the surface temperature through changing the SEB. In a previous study (Wang *et al* 2020), we presented the details of the SEB model and applied it to studying the cooling effectiveness of white roofs. Our new derivation and the key changes made in this study are presented in the supplementary materials (see text S2).

Based on the SEB model, the reduction in roof surface temperature due to green roof irrigation can be expressed as:

$$(\Delta T_s)_{\mathrm{SEB}} = \Delta Q' f = -\Delta \mathrm{LE} f = -L_v Q_{\mathrm{irrigation}} f \quad (1)$$

where ΔLE (W m^{-2}) is the difference in latent heat flux between an irrigated and a non-irrigated green roof, L_v (J kg^{-1}) is the latent heat of vaporization, $Q_{\mathrm{irrigation}}$ (kg m^{-2} s^{-1} or mm s^{-1}) is the irrigation water amount, and f (K W^{-1} m^2) is a surface energy redistribution factor $f = \frac{1}{\frac{1}{r_a'} + \frac{1}{r_g'} + \frac{1}{r_o'}}$ that encodes the efficiencies of different SEB components in transferring heat. The $1/r'_a$, $1/r'_g$, and $1/r'_o$ in f represent

the linearized heat transfer efficiencies (W m^{-2} K^{-1}) for convection, conduction (in this case conduction means heat transfer into the soil and the roof deck), and radiation, respectively. In our study, the daily mean CESM outputs are used as the input for the SEB model. For example, the $Q_{irrigation}$ term is taken from the well-irrigated scenario (Case_Irrigation), the ΔLE term is the change in the simulated latent flux between Case_Irrigation and Case_Noirrigation, and the f term is calculated based on equations S15–S18 in the supplementary materials using the CESM outputs from Case_Noirrigation.

A simple physical interpretation of equation (1) is that the latent heat flux boosted by irrigation is balanced by the reductions in sensible heat flux, ground heat flux, and outgoing longwave radiation, namely,

$$\Delta \mathrm{LE} = (-\Delta H) + (-\Delta G) + (-\Delta L_{\mathrm{out}}). \quad (2)$$

Since sensible heat flux, ground heat flux, and outgoing longwave radiation are all functions of surface temperature, it is the sum of their linearized efficiencies (i.e. $1/r'_a$, $1/r'_g$, and $1/r'_o$), or f, that determines the exact reduction of surface temperature in response to a change in latent heat flux caused by irrigation.

3. Results

3.1. Evaporative cooling benefits of green roof irrigation

We first focus on the land-only simulations and will discuss the land-atmosphere coupled simulations later. Figures in the main text show the annual (ANN) mean results, and the June, July, August (JJA) mean and December, January, February (DJF) mean results are presented in the supplementary materials. When the green roof is not irrigated, the cooling effect is weak due to the limited soil water availability (figures 2(a)–(c), S1(a)–(c), and S2(a)–(c)). In some regions, the green roof surface temperature and the 2 m air temperature even increase by 0 K–2 K. This is likely caused by the reduction in roof albedo. The green roof albedo value is a global constant (which is 0.3 in our simulations but can be adjusted by users), while the regular roof albedo values are from a global dataset (Jackson *et al* 2010) and are larger than 0.3 in many regions around the world. The reduction in roof albedo leads to the increased absorption of incoming shortwave radiation, and thus counteracts the evaporative cooling effects of green roofs under water stress conditions. On the other hand, when the green roof is well irrigated, the cooling effect is much stronger (figures 2(d)–(f), S1(d)–(f) and S2(d)–(f)): the surface temperature of green roofs is much lower than that of regular roofs with the majority of surface temperature difference ranging from −4 K to 0 K; and compared to the CTL case, the majority of 2 m air temperature reduction ranges from −1 K to 0 K. One can also see that the magnitude of cooling effects of green roof in summer (JJA for the Northern Hemisphere, and DJF for the Southern Hemisphere) is stronger than that in winter due to the stronger latent heat fluxes boosted by the higher solar irradiance. The underling physical mechanism will be further discussed in section 3.2.

To better understand the cooling benefits of green roof irrigation, we evaluate the difference of surface temperature of green roofs between the well-irrigated (Case_Irrigation) and non-irrigated (Case_Noirrigation) scenarios. We denote the reduction in green roof surface temperature simulated by the CESM model as $(\Delta T_s)_{\mathrm{CESM}}$, which shows strong spatial variability. The magnitude of $(\Delta T_s)_{\mathrm{CESM}}$ is large in regions like India, the Middle East and the North Africa at ANN and JJA mean scales (figures 3 and S3). In DJF, the Southern Hemisphere has larger $(\Delta T_s)_{\mathrm{CESM}}$ than the Northern Hemisphere (figure S4) but the magnitude of $(\Delta T_s)_{\mathrm{CESM}}$ in DJF is smaller than that in JJA.

The spatial pattern of the cooling benefits of green roof irrigation predicted by the SEB model (equation (1)) shows high correlations with the CESM results (figure 3). The R^2 values are 0.99 in ANN, JJA, and DJF (table 1). According to the SEB model (equation (1)), the two controlling factors are the irrigation amount multiplied by the latent heat of vaporization ($L_v \times Q_{\mathrm{irrigation}}$), and the surface energy redistribution factor (f) that encodes the efficiencies of different SEB components in transferring heat. We find that the spatial pattern of $(\Delta T_s)_{\mathrm{CESM}}$ is well correlated to $L_v \times Q_{\mathrm{irrigation}}$ with R^2 values of 0.93, 0.95 and 0.96 for ANN, JJA, and DJF, respectively. The spatial variation of f is much less important than that of $L_v \times Q_{\mathrm{irrigation}}$ in controlling the spatial variation of $(\Delta T_s)_{\mathrm{CESM}}$, at least based on the CESM results. The global mean value of f simulated by CESM is 0.035 ± 0.005 K W^{-1} m^2 for ANN, and it shows weak seasonal variations. The differences between the JJA/DJF results and the ANN results are less than 1.5% (figures S3 and S4).

3.2. Changes in the surface energy budget

In this section, we examine changes in the surface energy budget at the ANN mean scale. Results for JJA and DJF are again shown in the supplementary materials (figures S5–S8). In land-only simulations, the incoming shortwave and longwave radiation are not affected by the green roof irrigation; hence we only examine changes in sensible heat flux, latent heat flux, ground heat flux, and outgoing longwave radiation. We find that the increases in latent heat flux (ΔLE) are similar, in terms of magnitude and spatial pattern, to the decreases in sensible heat flux (ΔH) with R^2 values of 0.94, 0.98 and 0.96 for ANN, JJA, and DJF, respectively (cf figures 4(a) and

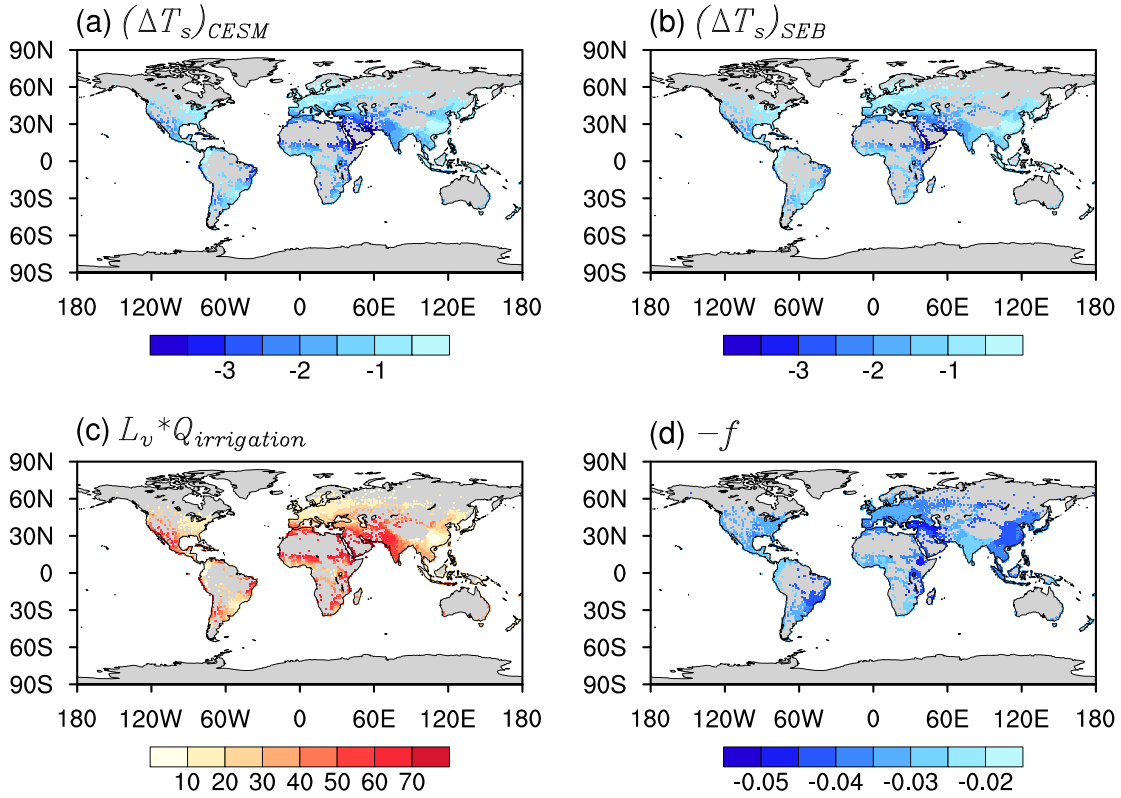

Figure 3. Surface temperature reduction due to green roof irrigation (unit: K) simulated by (a) CESM and predicted by (b) SEB. Also shown are (c) the irrigation water amount multiplied by the latent heat of vaporization (unit: W m^{-2}) and (d) the surface energy redistribution factor f (unit: K W^{-1} m^2). The irrigation water amount is from the Case_Irrigation output and the surface energy redistribution factor f is calculated based on equations S15–S18 in the supplementary materials using the Case_Noirrigation outputs. The results are the annual daily mean over 20 years (1991–2010) from land-only simulations. Only grid cells with more than 0.1% of urban land are shown.

(b)). We also find some reductions in ground heat flux (ΔG) and outgoing longwave radiation (ΔL_{out}), but they are much smaller than reductions in sensible heat flux (figures 4(c), (d) and 5(c), (d)). As a result, the increases in latent heat flux (ΔLE) are largely, although not entirely, balanced by the decreases in sensible heat flux (ΔH) (figure 5(b)). This result is also consistent with the findings of Sun *et al* (2016). Here we note that changes in the latent heat flux (ΔLE) and changes in other heat fluxes (e.g. ΔH, ΔG, and ΔL_{out}) tend to be linearly correlated because of the energy balance constraint, namely, $\Delta\text{LE} = (-\Delta H) + (-\Delta G) + (-\Delta L_{out})$. However, the exact relations between each other are quite complex and strongly depend on the green roof properties. The scattered and seemingly bifurcated relations between ΔLE and ΔG (figure 5(c)) are manifestation of the spatial variability of green roof properties.

We further find that the spatial pattern of ΔLE agrees well with that of $L_v \times Q_{irrigation}$ with R^2 values of 0.999, 0.997 and 0.994 for ANN, JJA, and DJF, respectively (cf figures 3(c) and 4(a) and see figure 5(a)). This indicates that most of irrigation water leaves the green roof system primarily through ET (see also figures S9–S11), which supports the assumption made in the SEB model. To further understand the main controlling factors of ΔLE, we find that the spatial pattern of ΔLE is more controlled by the insolation (S_{in}), with R^2 values of 0.54, 0.64 and 0.60 for ANN, JJA, and DJF, respectively, than the rainfall amount multiplied by the latent heat of vaporization ($L_v \times Q_{rain}$), implying that changes in ET under well irrigated conditions are more controlled by energy availability. This is consistent with the general understanding of ET dynamics (Brutsaert 1982).

In summary, green roof irrigation boosts the latent heat flux largely at the expense of sensible heat flux, and is mainly controlled by energy availability, not moisture availability from natural pathways (i.e. rainfall).

Table 1. The R^2 between the cooling benefits of green roof irrigation and their drivers for annual mean (ANN), JJA mean, and DJF mean over 20 years (1991–2010) from land-only simulations.

R^2	ANN	JJA	DJF
$(\Delta T_s)_{CESM}$ and $(\Delta T_s)_{SEB}$	0.99	0.99	0.99
$(\Delta T_s)_{CESM}$ and $(L_v \times Q_{irrigation})$	0.93	0.95	0.96
$(\Delta T_s)_{CESM}$ and f	0.04	0.12	0.01

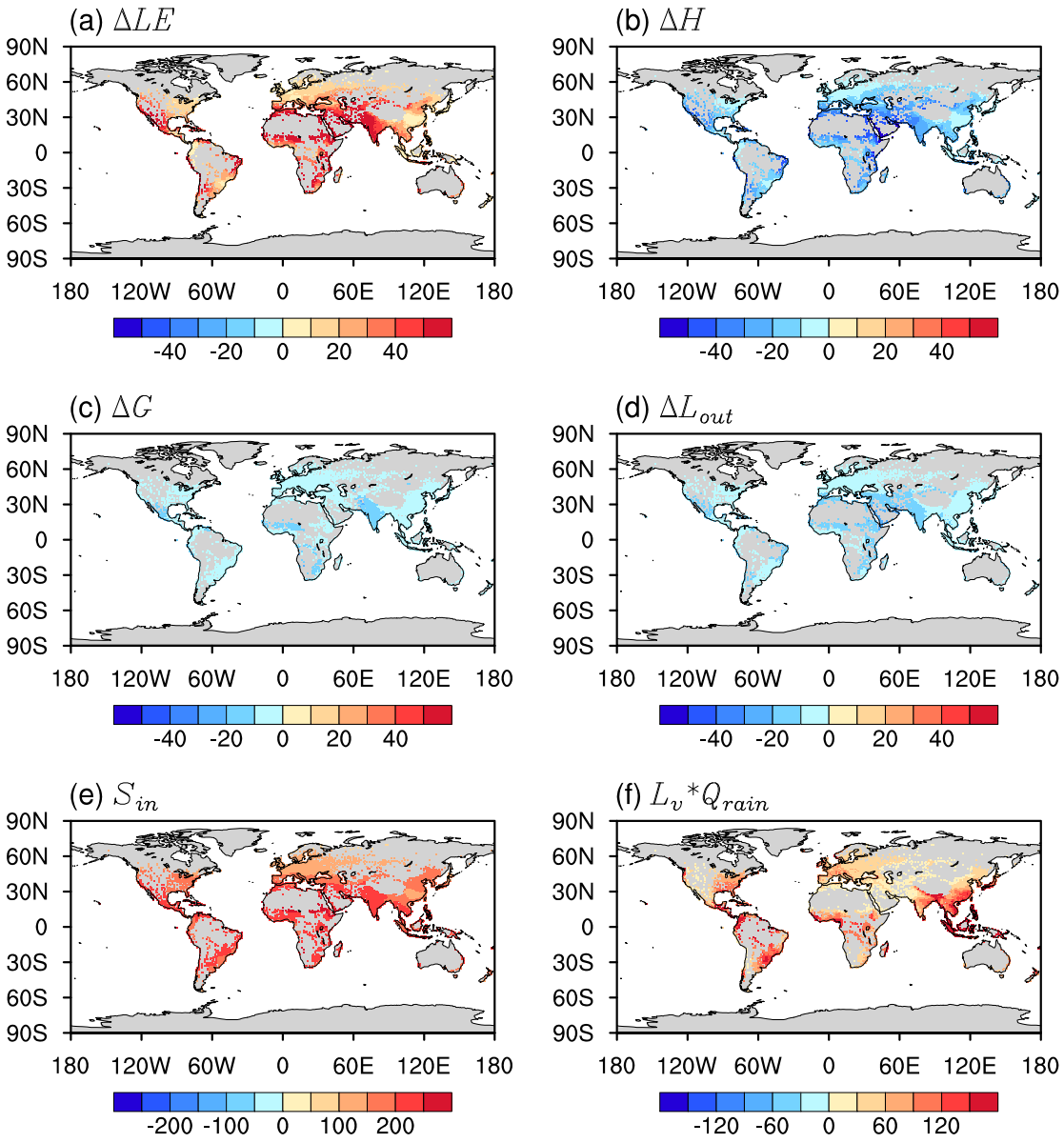

Figure 4. The changes in (a) latent heat flux, (b) sensible heat flux, (c) ground heat flux, and (d) outgoing longwave radiation due to green roof irrigation simulated by CESM. Also shown are the (e) insolation, and (f) precipitation multiplied by the latent heat of vaporization. All units are W m^{-2}. The results are the annual daily mean over 20 years (1991–2010) from land-only simulations. Only grid cells with more than 0.1% of urban land are shown.

3.3. Surface energy redistribution factor

It is not too surprising that the more irrigation is applied to the green roof, the more evaporative cooling benefits the green roof yields (namely, ΔT_s is highly correlated with $Q_{\text{irrigation}}$). However, a question that remains to be answered is what controls the ratio of $Q_{\text{irrigation}}$ to ΔT_s, which can be interpreted as the amount of irrigation water required to produce a unit decrease in green roof surface temperature. From equation (1) it can be shown that

$$\left(\frac{Q_{\text{irrigation}}}{\Delta T_s}\right)_{\text{SEB}} = -\frac{1}{L_v f} = \left(-\frac{1}{L_v r'_a}\right) + \left(-\frac{1}{L_v r'_g}\right) + \left(-\frac{1}{L_v r'_o}\right). \quad (3)$$

One can see that this new metric only depends on heat transfer efficiencies for convection, conduction, and radiation over green roofs.

Figure 6 shows the irrigation water amount per unit decrease of surface temperature as well as the contributions from each heat transfer mechanism. Compared to the other two heat transfer mechanisms, convection is the main driver of $\left(Q_{\text{irrigation}}/\Delta T_s\right)_{\text{SEB}}$. The annual mean of $-1/\left(L_v \times r'_a\right)$ is -0.56 ± 0.07 mm d^{-1} K^{-1} and contributes 55.3% to $\left(Q_{\text{irrigation}}/\Delta T_s\right)_{\text{SEB}}$. The contributions from conduction and radiation only account for 26.5% and 18.2%, respectively. Note that there exist some regions like India and West Africa where $-1/\left(L_v \times r'_g\right)$ is large and becomes comparable to $-1/\left(L_v \times r'_a\right)$. This is due to the large thermal

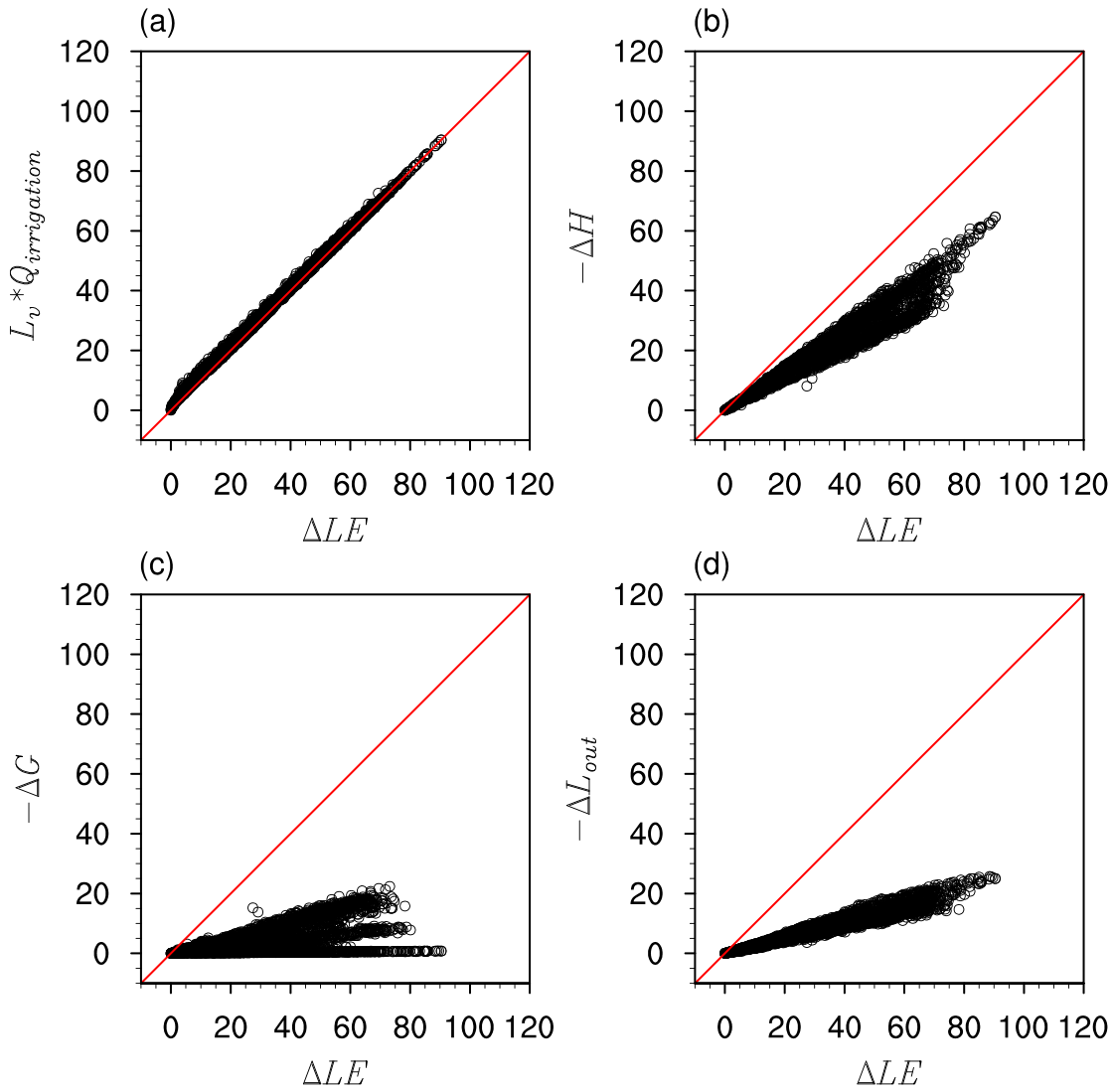

Figure 5. The relationship between the increase in latent heat flux and the (a) irrigation water amount multiplied by the latent heat of vaporization, (b) decrease in sensible heat flux, (c) decrease in ground heat flux, and (d) decrease in outgoing longwave radiation simulated by CESM. All units are W m^{-2}. The results are the annual daily mean over 20 years (1991–2010) from land-only simulations. Only grid cells with more than 0.1% of urban land are shown.

admittance of the roof deck prescribed by the input dataset (Jackson *et al* 2010, Oleson *et al* 2010), as discussed elsewhere (Wang *et al* 2020).

The $\left(Q_{\text{irrigation}}/\Delta T_s\right)_{\text{SEB}}$ and contributions from the different heat transfer mechanisms do not show large variations between JJA and DJF (figures S12 and S13). This can be explained by how the heat transfer efficiencies (i.e. $1/r'_a$, $1/r'_g$, and $1/r'_o$) are parameterized in CESM. The convective heat transfer efficiency $(1/r'_a)$ is primarily determined by the wind speed in the urban canopy layer (Oleson *et al* 2008a), which is slightly (1.5%) higher in DJF than in JJA due to the stable stratification that reduces the drag. The conductive heat transfer efficiency $(1/r'_g)$ is fully determined by the thermal admittance of the green roof system, including the soil layers and the roof deck. Since the roof deck properties do not change with time, the conductive heat transfer efficiency $(1/r'_g)$ only shows small seasonal variations as a result of variations in soil moisture. The efficiency for outgoing longwave radiation $(1/r'_o)$ is a function of the near-surface air temperature and hence exhibits the largest seasonal variations (decreases by 11.2% from JJA to DJF) among the three heat transfer efficiencies. However, since its contribution to $\left(Q_{\text{irrigation}}/\Delta T_s\right)_{\text{SEB}}$ is the smallest, its seasonal variations do not lead to large seasonal variations of $\left(Q_{\text{irrigation}}/\Delta T_s\right)_{\text{SEB}}$.

The importance of convective heat transfer efficiency, which represents the effect of atmospheric turbulence in transporting sensible heat, in controlling the irrigation amount is consistent with previous studies showing that wind is an important factor for ET in humid conditions (Santamouris 2014, Gunawardena *et al* 2017). The finding that the convective heat transfer efficiency is much stronger

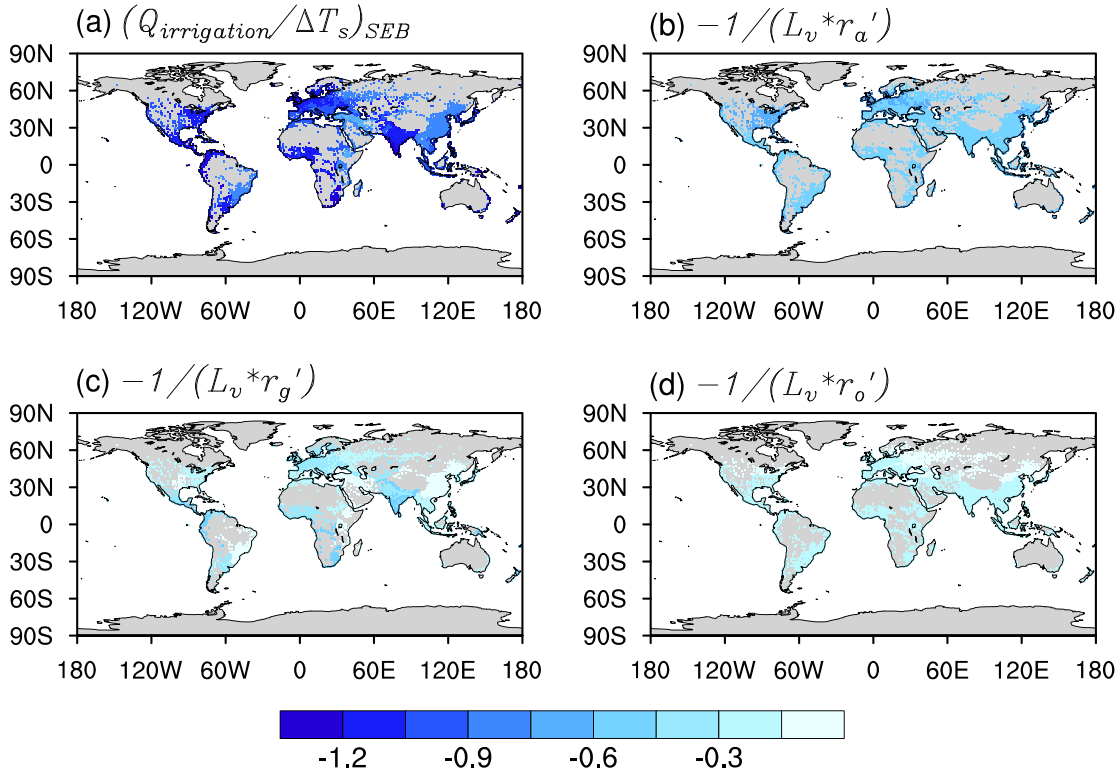

Figure 6. The SEB predicted (a) irrigation water demand per unit decrease of surface temperature for green roofs, and the individual contributions from the (b) convection, (c) conduction, and (d) radiation efficiencies. All units are mm d^{-1} K^{-1}. The results are the annual daily mean over 20 years (1991–2010) from land-only simulations. Only grid cells with more than 0.1% of urban land are shown.

than the other two efficiencies is consistent with a previous theoretical study (Bateni and Entekhabi 2012) and is also consistent with the results in figures 4 and 5 that the increases of latent heat fluxes are largely balanced by the decreases in sensible heat fluxes. The larger efficiency for convection implies that the sensible heat flux responds to perturbations (caused by irrigation) more strongly than the other two heat transfer mechanisms, as shown in figures 4 and 5. In the meantime, the decreases in sensible heat fluxes are related to the decreases in surface temperature through the convective heat transfer efficiency. Therefore, the convective heat transfer efficiency predominately controls the amount of irrigation water per unit decrease of green roof surface temperature, as shown in figure 6.

We point out that the values of $Q_{\text{irrigation}}/\Delta T_s$ reported here are different from those in Wang *et al* (2019). This is because we use different definitions of surface temperature and surface area. In our study, we are only concerned with the green roof system and hence the area is defined as the green roof area and the surface temperature is the green roof surface temperature. However, in Wang *et al* (2019), the study area is the grid cell size and the surface temperature is the surface temperature of the whole grid cell. Moreover, the study by Wang *et al* (2019) focuses on the effects of irrigation for ground vegetation with a much deeper soil layer. In their study, irrigation is applied to the top two soil layers with a total depth of 0.4 m. Therefore, not all irrigated water is used for ET since some water further infiltrates into deeper soils and/or generates runoff.

3.4. Land-atmosphere coupling

The above results are based on the land-only simulations. To examine whether the SEB model can be applied to the situation where the atmosphere responds to green roof irrigation at the same spatial resolution, we conduct land-atmosphere coupled simulations. The coupled simulations show that the cooling effects of green roof irrigation as well as the irrigation water demand per unit decrease of green roof surface temperature and their controlling factors change little compared to the land-only simulations (figures S14, S15 and table S4). Therefore, at the spatial resolutions used in our study, land-atmosphere coupling does not seem to alter our results. However, we recognize that this finding might not hold at other spatial resolutions (Li and Wang 2019). Further investigations with higher spatial resolutions are recommended to fully address the importance of land-atmosphere coupling.

4. Conclusion and discussion

In this study, we address the question of what controls the cooling benefits of green roof irrigation. We

find that green roof irrigation enhances ET or latent heat flux, which is largely balanced by the decrease of sensible heat flux. As a result, the amount of irrigation water required to produce a unit decrease of green roof surface temperature is strongly controlled by the convective heat transfer efficiency, which represents the capability of atmospheric turbulence in transferring sensible heat.

Our study highlights the importance of SEB in constraining the cooling benefits of green roof irrigation and is broadly consistent with previous theoretical and modelling studies (Bateni and Entekhabi 2012, Sun *et al* 2016). The findings of this study imply that to accurately predict the cooling benefits of green roof irrigation, we need better parameterizations for convective heat transfer within and over urban canopies. This is consistent with a recent review study (Krayenhoff *et al* 2021) reporting that uncertainties in key physical processes such as heat convection and conduction contribute to the large range of rooftop heat mitigation effectiveness. Currently the convective heat transfer efficiency for roofs in CLMU is parameterized as a function of the wind speed in the urban canopy layer, which can be traced to earlier work in the 1930s (Rowley *et al* 1930, Rowley and Eckley 1932). The uncertainties (maybe even flaws) in this parameterization, which further relies on the parameterization of wind profile in the canopy layer, will be reflected in the convective heat transfer efficiency. The parameterization of convective heat transfer efficiency for urban surfaces continues to be a grand challenge (Hagishima *et al* 2005), but high-fidelity large-eddy simulations might shed some insights into this issue (Li *et al* 2016).

Our work not only improves the understanding of energy and water balances of green roofs, but also provides valuable guidance for urban planners and policy makers in terms of heat mitigation and sustainable water management. In water-scare regions, estimating the amount of irrigation water needed for green infrastructures is an important step for assessing their viability and effectiveness (Van Mechelen *et al* 2015, Wang *et al* 2019). Due to the complex interactions of many factors (e.g. climatic conditions, vegetation characteristics, green roof structure and materials, and irrigation strategies), previous studies often relied on numerical modelling to quantify the trade-off between heat mitigation and water conservation for green infrastructures. Using simple water and energy balance arguments aided by a global Earth System Model, our work demonstrates that the amount of irrigation water needed by green roofs to achieve a reduction of one degree in the green roof surface temperature, i.e. $\left(Q_{\text{irrigation}}/\Delta T_{\text{s}}\right)_{\text{SEB}}$, is reasonably constrained. The key to minimize the irrigation amount per unit decrease of green roof surface temperature is to reduce the heat transfer efficiencies for convection, conduction, and radiation. This further implies that we should try to put green roofs in places with lower wind speed (i.e. smaller convective heat transfer efficiency) and use green roof materials that have smaller heat capacity and thermal conductivity (i.e. smaller conductive heat transfer efficiency). The heat transfer efficiency for radiation is dependent on the near-surface air temperature and its contribution to $\left(Q_{\text{irrigation}}/\Delta T_{\text{s}}\right)_{\text{SEB}}$ is limited; hence its policy implication is not highlighted here.

As alluded to earlier, the aim of this study is not to predict the water use of green roofs globally, but rather to demonstrate how irrigation changes the energy balance over green roofs thereby altering the surface temperature of green roofs. Hence our approach is different from many previous studies that focused on developing detailed parameterizations for green roofs including sophisticated irrigation schemes. Our approach is intended to complement and not replace city-specific case studies that are needed to assess the local-scale benefits of green roof irrigation and to avoid the negative impacts on the potentially scarce water resources. The green roof parameterization implemented into CLMU is a compromise between including enough ingredients for studying green roofs but also maintaining maximum consistency with the original CLMU in terms of model structure and calculation. Other factors like vegetation types and spectral characteristics, substrate types, as well as other material composition (Kolokotsa *et al* 2013, Santamouris 2014, Starry *et al* 2014) have not been fully considered by the parameterization used in this study. The irrigation scheme is also simplified. From the perspective of water and energy balances, our key assumption is that the irrigated water does not produce too much runoff, which seems to be supported by the CESM results (figures S9–S11). This does not mean that the green roof does not produce any runoff. Rather, it means that most of the added water through irrigation does not leave the green roof system through runoff, but through ET. In reality, this may or may not be true but could be achieved with proper design and scheduling of irrigation. Future studies using realistic irrigation schedules (e.g. investigating the actual water requirements by the vegetation) are highly recommended. We note, however, that even if our assumption was not valid, our results allow one to estimate the upper limit of cooling benefits provided by green roof irrigation (i.e. when all irrigated water leaves the green roof system through ET). We also point out that we primarily deal with the green roof surface temperature in this study. Although the effects on the 2 m air temperature are presented (figure 2), more detailed investigations on the near-surface air temperature and other boundary layer quantities are left for future studies.

Data availability statement

The data that support the findings of this study are openly available at the following URL/DOI: http://doi.org/10.5281/zenodo.4482784.

Acknowledgments

This research was supported by the U.S. Department of Energy, Office of Science, as part of research in Multi-Sector Dynamics, Earth and Environmental System Modelling Program. We would like to acknowledge high-performance computing support from Cheyenne (http://doi.org/10.5065/D6RX99HX) provided by NCAR's Computational and Information Systems Laboratory, as well as National Energy Research Scientific Computing Center (NERSC) which is a U.S. Department of Energy Office of Science User Facility operated under Contract No. DE-AC02-05CH11231, to run CESM. We also thank Dr Ting Sun at University of Reading and Professor Guangheng Ni at Tsinghua University for providing the field measurements. The authors declare no competing financial interests. CESM/CLM5 release code (tag: release-cesm2.0.02) is available at www.cesm.ucar.edu/models/cesm2/release_download.html.

ORCID iDs

Linying Wang https://orcid.org/0000-0003-0876-9220
Dan Li https://orcid.org/0000-0001-5978-5381

References

Bateni S M and Entekhabi D 2012 Relative efficiency of land surface energy balance components *Water Resour. Res.* **48** W04510
Besir A B and Cuce E 2018 Green roofs and facades: a comprehensive review *Renew. Sustain. Energ. Rev.* **82** 915–39
Brutsaert W 1982 *Evaporation into the Atmosphere: Theory, History and Applications* (Heidelberg: Springer)
Chagolla-Aranda M A, Simá E, Xamán J, Álvarez G, Hernández-Pérez I and Téllez-Velázquez E 2017 Effect of irrigation on the experimental thermal performance of a green roof in a semi-warm climate in Mexico *Energy Build.* **154** 232–43
Danabasoglu G *et al* 2020 The Community Earth System Model Version 2 (CESM2) *J. Adv. Model. Earth Syst.* **12** e2019MS001916
DiGiovanni K, Montalto F, Gaffin S and Rosenzweig C 2013 Applicability of classical predictive equations for the estimation of evapotranspiration from urban green spaces: green roof results *J. Hydrol. Eng.* **18** 99–107
Epstein S A, Lee S M, Katzenstein A S, Carreras-Sospedra M, Zhang X, Farina S C, Vahmani P, Fine P M and Ban-Weiss G 2017 Air-quality implications of widespread adoption of cool roofs on ozone and particulate matter in southern California *Proc. Natl Acad. Sci. USA* **114** 8991–6
Estrada F, Botzen W J W and Tol R S J 2017 A global economic assessment of city policies to reduce climate change impacts *Nat. Clim. Change* **7** 403–6
Gaffin S R, Khanbilvardi R and Rosenzweig C 2009 Development of a green roof environmental monitoring and meteorological network in new york city *Sensors* **9** 2647–60
Gagliano A, Detommaso M, Nocera F and Berardi U 2016 The adoption of green roofs for the retrofitting of existing buildings in the Mediterranean climate *Int. J. Sustain. Build. Technol. Urban Dev.* **7** 116–29
Gates W L *et al* 1999 An overview of the results of the atmospheric model intercomparison project (AMIP I) *Bull. Am. Meteorol. Soc.* **80** 29–56
Georgescu M 2015 Challenges associated with adaptation to future urban expansion *J. Clim.* **28** 2544–63
Georgescu M, Morefield P E, Bierwagen B G and Weaver C P 2014 Urban adaptation can roll back warming of emerging megapolitan regions *Proc. Natl Acad. Sci. USA* **111** 2909–14
Gunawardena K R, Wells M J and Kershaw T 2017 Utilising green and bluespace to mitigate urban heat island intensity *Sci. Total Environ.* **584–585** 1040–55
Hagishima A, Tanimoto J and Narita K-I 2005 Intercomparisons of experimental convective heat transfer coefficients and mass transfer coefficients of urban surfaces *Bound. Layer Meteorol.* **117** 551–76
He Y, Yu H, Ozaki A, Dong N and Zheng S 2017 Long-term thermal performance evaluation of green roof system based on two new indexes: a case study in Shanghai area *Build. Environ.* **120** 13–28
Heusinger J, Sailor D J and Weber S 2018 Modeling the reduction of urban excess heat by green roofs with respect to different irrigation scenarios *Build. Environ.* **131** 174–83
Jackson T L, Feddema J J, Oleson K W, Bonan G B and Bauer J T 2010 Parameterization of urban characteristics for global climate modeling *Ann. Am. Assoc. Geogr.* **100** 848–65
Jarvis P G, Monteith J L and Weatherley P E 1976 The interpretation of the variations in leaf water potential and stomatal conductance found in canopies in the field *Phil. Trans. R. Soc.* B **273** 593–610
Kolokotsa D, Santamouris M and Zerefos S C 2013 Green and cool roofs' urban heat island mitigation potential in European climates for office buildings under free floating conditions *Sol. Energy* **95** 118–30
Krayenhoff E S, Broadbent A M, Zhao L, Georgescu M, Middel A, Voogt J A, Martilli A, Sailor D J and Erell E 2021 Cooling hot cities: a systematic and critical review of the numerical modelling literature *Environ. Res. Lett.* **16** 053007
Lawrence D M *et al* 2019 The community land model version 5: description of new features, benchmarking, and impact of forcing uncertainty *J. Adv. Model. Earth Syst.* **11** 4245–87
Li D, Bou-Zeid E and Oppenheimer M 2014 The effectiveness of cool and green roofs as urban heat island mitigation strategies *Environ. Res. Lett.* **9** 055002
Li D and Wang L 2019 Sensitivity of surface temperature to land use and land cover change-induced biophysical changes: the scale issue *Geophys. Res. Lett.* **46** 9678–89
Li Q, Bou-Zeid E, Anderson W, Grimmond S and Hultmark M 2016 Quality and reliability of LES of convective scalar transfer at high Reynolds numbers *Int. J. Heat Mass Transfer* **102** 959–70
Ng E, Chen L, Wang Y and Yuan C 2012 A study on the cooling effects of greening in a high-density city: an experience from Hong Kong *Build. Environ.* **47** 256–71
Oke T R, Mills G, Christen A and Voogt J A 2017 *Urban Climates* (Cambridge: Cambridge University Press)
Oleson K W 2012 Contrasts between urban and rural climate in CCSM4 CMIP5 climate change scenarios *J. Clim.* **25** 1390–412
Oleson K W, Bonan G B and Feddema J 2010 Effects of white roofs on urban temperature in a global climate model *Geophys. Res. Lett.* **37** L03701
Oleson K W, Bonan G B, Feddema J and Jackson T 2011 An examination of urban heat island characteristics in a global climate model *Int. J. Climatol.* **31** 1848–65

Oleson K W, Bonan G B, Feddema J and Vertenstein M 2008b An urban parameterization for a global climate model. Part II: sensitivity to input parameters and the simulated urban heat island in offline simulations *J. Appl. Meteorol. Climatol.* **47** 1061–76

Oleson K W, Bonan G B, Feddema J, Vertenstein M and Grimmond C S B 2008a An urban parameterization for a global climate model. Part I: formulation and evaluation for two cities *J. Appl. Meteorol. Climatol.* **47** 1038–60

Oleson K W and Feddema J 2020 Parameterization and surface data improvements and new capabilities for the Community Land Model Urban (CLMU) *J. Adv. Model. Earth Syst.* **12** e2018MS001586

Qin H-P, Peng Y-N, Tang Q-L and Yu S-L 2016 A HYDRUS model for irrigation management of green roofs with a water storage layer *Ecol. Eng.* **95** 399–408

Rowley F B, Algren A B and Blackshaw J L 1930 Surface conductances as affected by air velocity, temperature and character of surface *ASHRAE Trans.* **36** 429–46

Rowley F B and Eckley W A 1932 Surface coefficients as affected by wind direction *ASHRAE Trans.* **38** 33–46

Sailor D J 2008 A green roof model for building energy simulation programs *Energy Build.* **40** 1466–78

Santamouris M 2014 Cooling the cities—a review of reflective and green roof mitigation technologies to fight heat island and improve comfort in urban environments *Sol. Energy* **103** 682–703

Scholz-Barth K and Tanner S 2004 *Green Roofs: Federal Energy Management Program (FEMP) Federal Technology Alert* (Golden, CO: National Renewable Energy Lab)

Shafique M, Kim R and Rafiq M 2018 Green roof benefits, opportunities and challenges—a review *Renew. Sustain. Energ. Rev.* **90** 757–73

Sharma A, Conry P, Fernando H J S, Hamlet A F, Hellmann J J and Chen F 2016 Green and cool roofs to mitigate urban heat island effects in the Chicago metropolitan area: evaluation with a regional climate model *Environ. Res. Lett.* **11** 064004

Smith K R and Roebber P J 2011 Green roof mitigation potential for a proxy future climate scenario in Chicago, Illinois *J. Appl. Meteorol. Climatol.* **50** 507–22

Song J, Wang Z-H and Wang C 2018 The regional impact of urban heat mitigation strategies on planetary boundary layer dynamics over a semiarid city *J. Geophys. Res. Atmos.* **123** 6410–22

Starry O, Lea-Cox J D, Kim J and Van Iersel M W 2014 Photosynthesis and water use by two Sedum species in green roof substrate *Environ. Exp. Bot.* **107** 105–12

Sun T, Bou-Zeid E and Ni G-H 2014 To irrigate or not to irrigate: analysis of green roof performance via a vertically-resolved hygrothermal model *Build. Environ.* **73** 127–37

Sun T, Bou-Zeid E, Wang Z-H, Zerba E and Ni G-H 2013 Hydrometeorological determinants of green roof performance via a vertically-resolved model for heat and water transport *Build. Environ.* **60** 211–24

Sun T, Grimmond C S B and Ni G-H 2016 How do green roofs mitigate urban thermal stress under heat waves? *J. Geophys. Res. Atmos.* **121** 5320–35

Tian Y, Bai X, Qi B and Sun L 2017 Study on heat fluxes of green roofs based on an improved heat and mass transfer model *Energy Build.* **152** 175–84

Tsang S W and Jim C Y 2011 Theoretical evaluation of thermal and energy performance of tropical green roofs *Energy* **36** 3590–8

Tsang S W and Jim C Y 2016 Applying artificial intelligence modeling to optimize green roof irrigation *Energy Build.* **127** 360–9

Vahmani P and Hogue T S 2014 Incorporating an urban irrigation module into the Noah land surface model coupled with an urban canopy model *J. Hydrometeorol.* **15** 1440–56

Vahmani P and Hogue T S 2015 Urban irrigation effects on WRF-UCM summertime forecast skill over the Los Angeles metropolitan area *J. Geophys. Res. Atmos.* **120** 9869–81

Vahmani P and Jones A D 2017 Water conservation benefits of urban heat mitigation *Nat. Commun.* **8** 1072

Van Heerwaarden C C and Teuling A J 2014 Disentangling the response of forest and grassland energy exchange to heatwaves under idealized land-atmosphere coupling *Biogeosciences* **11** 6159–71

Van Mechelen C, Dutoit T and Hermy M 2015 Adapting green roof irrigation practices for a sustainable future: a review *Sustain. Cities Soc.* **19** 74–90

Wang C, Wang Z-H and Yang J 2019 Urban water capacity: irrigation for heat mitigation *Comput. Environ. Urban Syst.* **78** 101397

Wang L, Huang M and Li D 2020 Where are white roofs more effective in cooling the surface? *Geophys. Res. Lett.* **47** e2020GL087853

Wang Z-H, Bou-Zeid E and Smith J A 2013 A coupled energy transport and hydrological model for urban canopies evaluated using a wireless sensor network *Q. J. R. Meteorol. Soc.* **139** 1643–57

WGIN 2021 World green infrastructure network (WGIN) (available at: https://worldgreeninfrastructurenetwork.org/global-network/) (accessed 4 June 2021)

William R, Goodwell A, Richardson M, Le P V V, Kumar P and Stillwell A S 2016 An environmental cost-benefit analysis of alternative green roofing strategies *Ecol. Eng.* **95** 1–9

Wong N H, Chen Y, Ong C L and Sia A 2003 Investigation of thermal benefits of rooftop garden in the tropical environment *Build. Environ.* **38** 261–70

Yang J and Wang Z-H 2015 Optimizing urban irrigation schemes for the trade-off between energy and water consumption *Energy Build.* **107** 335–44

Yang J and Wang Z-H 2017 Planning for a sustainable desert city: the potential water buffering capacity of urban green infrastructure *Landscape Urban Plan.* **167** 339–47

Yang J, Wang Z-H, Chen F, Miao S, Tewari M, Voogt J A and Myint S 2015 Enhancing hydrologic modelling in the coupled weather research and forecasting–urban modelling system *Bound. Layer Meteorol.* **155** 87–109

Zinzi M and Agnoli S 2012 Cool and green roofs. An energy and comfort comparison between passive cooling and mitigation urban heat island techniques for residential buildings in the Mediterranean region *Energy Build.* **55** 66–76